Journal of Hydraulic Research Vol. 48, No. 1 (2010), pp. 23–32
doi:10.1080/00221680903568600

esearch paper

low movement and sediment transport in compound channels

HUNHONG HU (IAHR Member), Professor, Vice President, *China Institute of Water Resources and Hydropower esearch (IWHR); Secretary General, International Research and Training Center on Erosion and Sedimentation, ijing 100048, People's Republic of China.*
nail: huch@iwhr.com

JWEN JI, Professor, *IWHR, Beijing 100048, People's Republic of China.*
nail: jzw@iwhr.com

NGCHAO GUO (IAHR Member), Professor, *IWHR, Beijing 100048, People's Republic of China.*
nail: guoq@iwhr.com (author for correspondence)

STRACT
ere are many studies on the flow movement in compound channels, yet few are concerned with sediment transport. An experimental study on the flow vement and sediment transport in compound channels is presented. The experimental results indicate that the distribution of longitudinal velocity h depth in the main channel and the floodplains has a logarithmic component. The longitudinal velocity with flow depth in the interactive region does obey a logarithmic distribution, but involves a wake function. In the boundary region, the longitudinal velocity obeys a parabolic distribution. In lition, based on the suspended sediment diffusion equation and the flow interaction between main channel and floodplains, expressions are derived to dict the lateral eddy viscosity and the sediment diffusion coefficients. Finally, an analytical solution for the lateral distribution of the depth-averaged ocity and sediment concentration in a compound channel is obtained. The results from the analytical solution agree well with experimentation.

ywords: Compound channel, floodplain, flow exchange, main channel, sediment concentration distribution, velocity distribution

Introduction

erbank flow is a common phenomenon in fluvial rivers. If the charge is small, flow runs in the main channel, while the flow ers the floodplains otherwise. The flow characteristics of comnd channels, such as the flow conveying capacity, flow struc- and distribution of sediment concentration, have been lied since the 1970s. Myers (1978), Wormleaton *et al.* 82), and Prinos and Townsend (1984) considered the disrge calculated using the "single channel"-method which found 16–40% smaller than from observations, and that error gradually increases with the resistance in the main nnel and floodplain. Prinos and Townsend (1984), Ervine Baird (1982), and Wormleaton and Merrett (1990) suggested the main channel and floodplain should be treated separately. total discharge was calculated by summing the discharges of various subsections. The estimated discharge is more accu- if the apparent shear stress between the main channel and dplain is considered (Fukuhara and Murota 1990). Tominaga *et al.* (1991, 1993) analysed the turbulence intensity at the interface of the main channel and floodplain under different roughness and depth conditions. Knight and Shiono (1990) proposed experimental formulas to estimate the turbulence intensity. Myers (1978) suggested that the momentum transfer from channel to floodplain can be taken as an apparent shear force, and its maximum value may reach 25% of the weight of the main channel water component. Experiments conducted by Tominaga and Nezu (1991) and Rajaratnam and Ahmadi (1981) indicated that the maximum bed shear stresses in the main channel and floodplains are near the centre and their interface, respectively. Compared with a single channel, the shear stress in a compound channel decreases in the main channel but increases in the floodplain (Myers and Elsawy 1975, Myers 1978).

Rhodes and Knight (1994), Rajaratnam and Ahmadi (1981) and Ji (1997) recorded the flow velocity. They deduced that the vertical velocity distribution is deformed by momentum transfer and an obvious departure from the logarithmic law was observed

sion received 2 September 2009/Open for discussion until 31 August 2010.

0022-1686 print/ISSN 1814-2079 online
/www.informaworld.com

in both the main channel and the floodplain. Xie (1980), Zhou (1995), Ji (1997), and Shiono and Knight (1991) presented analytical results on the transverse distribution of the depth-averaged velocity according to the kinetic flow equation. James (1985) and Liu (1991) simulated the distribution of sediment concentration using numerical models. Many results for the flow movement are currently available, but few works of research on sediment transport in compound channels can be found. This research generalizes the river reaches into two types: straight and the lotus-root-shape compound channels that describe common natural fluvial rivers for which experiments on the flow movement and the sediment transport are conducted.

2 Experimental methodology

2.1 *Experimental conditions*

In this research, the generalized physical model includes straight and lotus-root-shape models 30 m in length. A self-circulating structure was adopted in the model, and both sides and beds were fixed with smooth cement. The values of Manning roughness coefficients for the main channel and the floodplains were 0.011 and 0.013 $s/m^{1/3}$, respectively. The symmetrical cross-sections consist of one channel and two floodplains, and the bed slope was 0.001. For the straight channel, the width of the main channel was $b = 0.3$ m and the width of the floodplain $(B - b)/2 = 0.35$ m. Here B is the width of compound channel. The height difference between the channel and floodplain was $h_d = 0.06$ m. For the lotus-root-shape channel, $b =$ 0.3 m; however, $(B - b)/2$ changes from 0 to 0.35 m. The length of each lotus-root-shape reach is 4 m. There is a 1 m transitional reach between each lotus-root-shape reach (Fig. 1). Data were collected in seven cross-sections in a lotus-root-shape reach, but only the fourth cross-section has the same dimension as the straight channel. The data from this cross-section were used as the comparison between the two channels.

The experimental reach is 20 m long and extends from downstream of the model inlet to 3 m upstream of the o Owing to channel symmetry, the measurements were taken for a half cross-section from the channel axis to one ch side. Ten to fifteen vertical lines, of which each line has 5 nodes, were used to measure velocity and sediment concentra The cross-section for measuring velocity and sediment co tration was 18 m downstream of the inlet. Experiments were ducted in the two channels under various flow and sedi conditions. Selected experimental conditions are liste Table 1, including discharge, flow depth, velocity, Fr number $\mathsf{F} = U/(gH)^{1/2}$, where g is the gravitational acceler and Reynolds number $\mathsf{R} = UH/\nu$, where ν is the kinematic cosity. For experiments in the straight channel, the flow and ment conditions included the flow depth of the main ch (subscript *mc*) $H_{mc} = 0.025$–0.127 m, the discharge and sedi concentration at the inlet, $Q = 0.002$–0.039 m^3/s and 4–83 kg/m^3, respectively. For experiments in the lotus-shape channel, $H_{mc} = 0.030$–0.122 m, $Q = 0.009$–0.022 r and suspended sediment concentration was $S = 4$–25 kg Ash from burnt coal was used as model sand, with a median d eter of $d_{50} = 1.4 \times 10^{-5}$ m and specific gravity of 2100 kg/m^3 subscript "*fp*" used in Fig. 1 and Table 1 describes the flood

2.2 *Instrumentation*

Velocity measurements were undertaken with an indu pressure measurement set. The equipment comprise guiding-pressure system, an inductive system and a magni system. As the inductive probes are subjected by a flow pres a film resistor in the inductive probe transfers the distortion the pressure difference into an electric signal. A steady ele pressure can be output by compensating and magni modes. Therefore, flow velocity can be measured depen on the calibrated linear relationship between output ele pressure and the acting flow force.

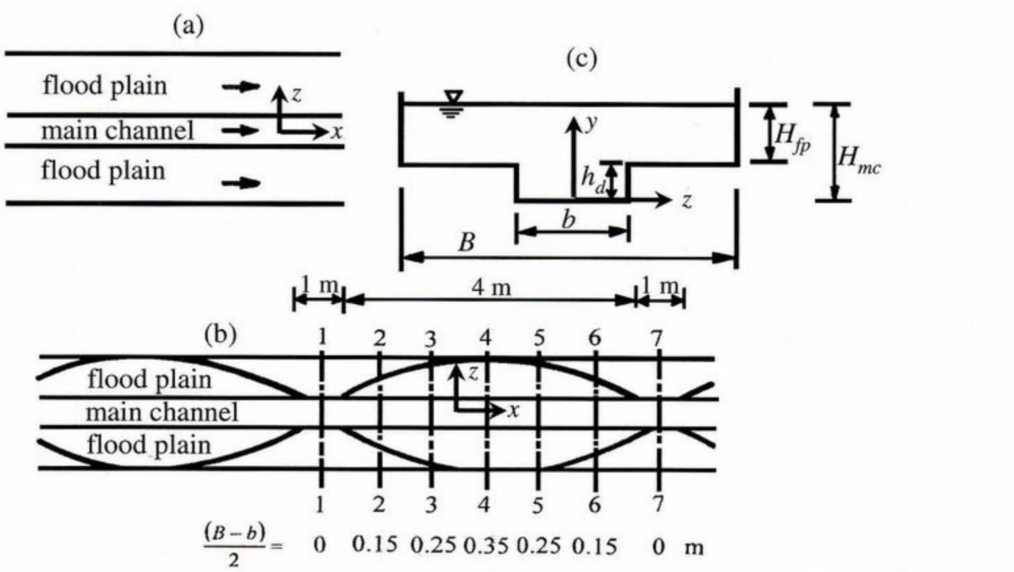

Figure 1 Sketches of (a) straight and (b) lotus-root-shape compound channels, (c) compound cross section

ble 1 Main experimental variables

n no.	Q (m³/s)	H_{mc} (m)	H_{fp} (m)	U_{mc} (m/s)	U_{fp} (m/s)	F_{mc}	F_{fp}	R_{mc}	R_{fp}
	0.017	0.091	0.031	0.119	0.066	0.13	0.12	10,703	2304
	0.022	0.100	0.040	0.134	0.090	0.14	0.14	13,377	3614
	0.026	0.108	0.048	0.148	0.110	0.14	0.16	15,778	5175
	0.033	0.116	0.056	0.179	0.152	0.17	0.20	20,637	8468
	0.039	0.127	0.067	0.199	0.187	0.18	0.23	25,074	12,452

Two methods were applied to measure the sediment concen-ıtion. An ultrasonic apparatus was used for concentrations ;s than 15 kg/m^3, otherwise pycnometers were used. The accu-:y for the sediment concentration measurement was 0.1 kg/m^3.

Analysis of experimental data

l Flow conveying capacity

ıe relationships between water level and discharge in the aight and lotus-root-shape compound channels are shown in g. 2. The relationship between water level and discharge in a ıgle channel without floodplains is also shown in Fig. 2, as cal-lated using Manning's formula by assuming identical depth d area as for the two compound channels. Because of the omentum transfer between the main channel and the flood-ains, the flow conveying capacity in the straight channel is ;s than that in a single channel, but larger than that in the us-root-shape channel, with their differences increasing adually with the flow depth. With a relative depth of floodplain main channel $H_{fp}/H_{mc} = 0.14{-}0.51$, flow conveying pacities in the straight and lotus-root-shape compound chan-ls decreased by 7–21%, and 11–48%, respectively, compared th the single channel capacity. In addition, the flow conveying pacity in the lotus-root-shape compound channel is 4–34% ;s than that in the straight compound channel.

! Distribution of flow velocity

is seen from Fig. 3 that the tendencies of the cross-sectional ıan velocity are similar for the two compound channels.

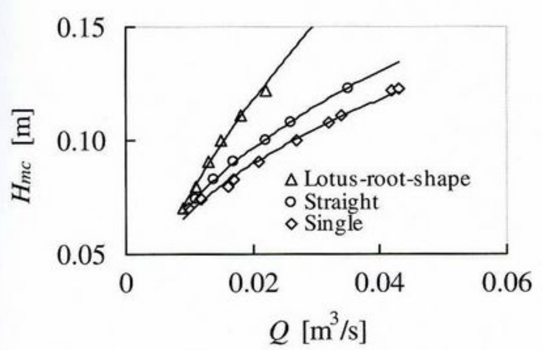

Figure 2 Depth-discharge relationships of channels investigated

With increasing depth, the mean velocities in the main channel first increase, then decrease and rise again, whereas the velocities in the floodplain continually increase. This kind of distribution indicates that momentum transfer exists between the main channel and the floodplains. The difference in distributions means that the momentum transfer is stronger in the lotus-root-shape channel than in the straight channel. The relative velocity of floodplain to channel U_{fp}/U_{mc} increases with relative depth H_{fp}/H_{mc}, and the velocities are largely different at lower relative depth, but similar at a higher relative depth, as shown in Fig. 4.

Distributions of depth-averaged velocity are shown in Fig. 5. For different depths, distributions in the two compound channels are similar, and the depth-averaged velocities decrease gradually

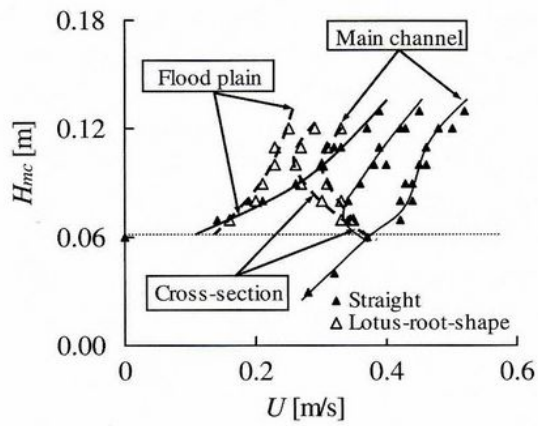

Figure 3 Depth-velocity relationships of two compound channels

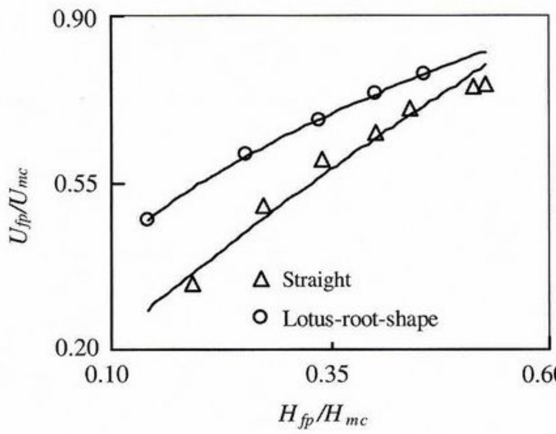

Figure 4 Relationships between relative depth and velocity for floodplain and channel

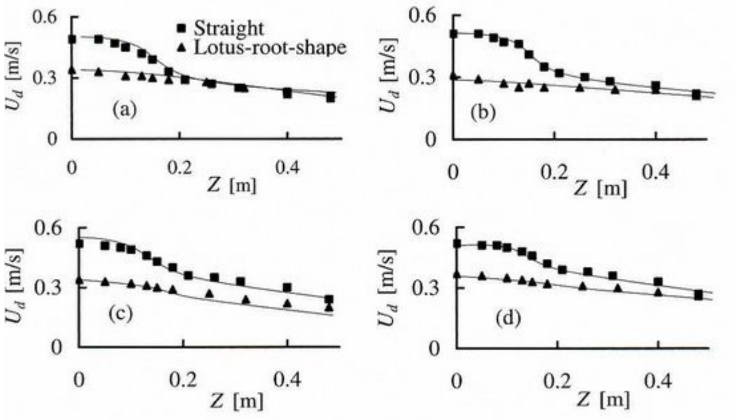

igure 5 Transverse distributions of depth-averaged velocity for H_{mc} = (a) 0.09 m, (b) 0.10 m, (c) 0.11 m, and (d) 0.12 m

:om the central zone of the main channel to the sides of the oodplains, although some differences are observed. First, the ifference between the maximum and minimum velocities and ıe transverse gradient of velocity near the interface are larger ı the straight channel than in the lotus-root-shape channel. econd, the differences in depth-averaged velocity are obvious ı the main channel zones, but the opposite is true in the oodplains.

Research by Rajaratnam and Ahmadi (1981), Rhodes and ͡night (1994), Xie (1980), Zhou (1995) or Shiono and Knight 1991) indicates that the distributions of depth-averaged velocity ave characteristics common with the present research. In ;eneral, the peak value of the momentum transfer appears near ıe interface of the main channel and the floodplain, where the :ansverse gradient of the velocity reaches a maximum. If the hannel and floodplain are broad enough, a region may exist in /hich the transverse gradient approaches zero in the main hannel and floodplain zones, and flow movement would not e affected by momentum transfer in these zones. The momen-ım transfer greatly affects the flow movement in the transition region between these two zones. This region is a keysto the study of overbank flow, therefore.

The non-dimensional velocity distributions are shov Fig. 6 for typical data sets. Most vertical distributions obe logarithmic distribution law, except near the channel/flooc interface. The distributions near this interface exhibit distortion. At the main channel side, the locations of maxi velocity are not at the flow surface, but at a lower point. / floodplain side, the maximum velocity is still at the surface. The distributions obey the logarithmic law if the in the floodplain is less than ϕh. Here, coefficient ϕ between 0.5 and 1.0 in the main channel and 0.2–1.0 i floodplain. The coefficient ϕ reaches a minimum at the inte and increases gradually to a maximum from the interfa the central zones of the floodplain and the main channel. depth in the floodplain is larger than ϕh, the distributioı not obey the logarithmic law. At the side of the main chа the measured velocities are always smaller than calcu from the logarithmic formula. On the other hand, at the f plain side, the measured velocities are always greater these calculated. The differences between measured and c lated velocities exhibits two characteristics: (1) maximum c ence in the transverse direction appears near the cha floodplain interface and decreasing in either direction froı interface; and (2) maximum difference in the vertical dire is observed at the flow surface, and differences almost disap if the depth is equal to ϕh.

3.3 *Distribution of sediment concentration*

For the two compound channels, the mean sediment co tration in the floodplain was smaller than in the main chа The relationships between the relative sediment concentı S_{fp}/S_{mc}, the relative velocity U_{fp}/U_{mc} and the relative

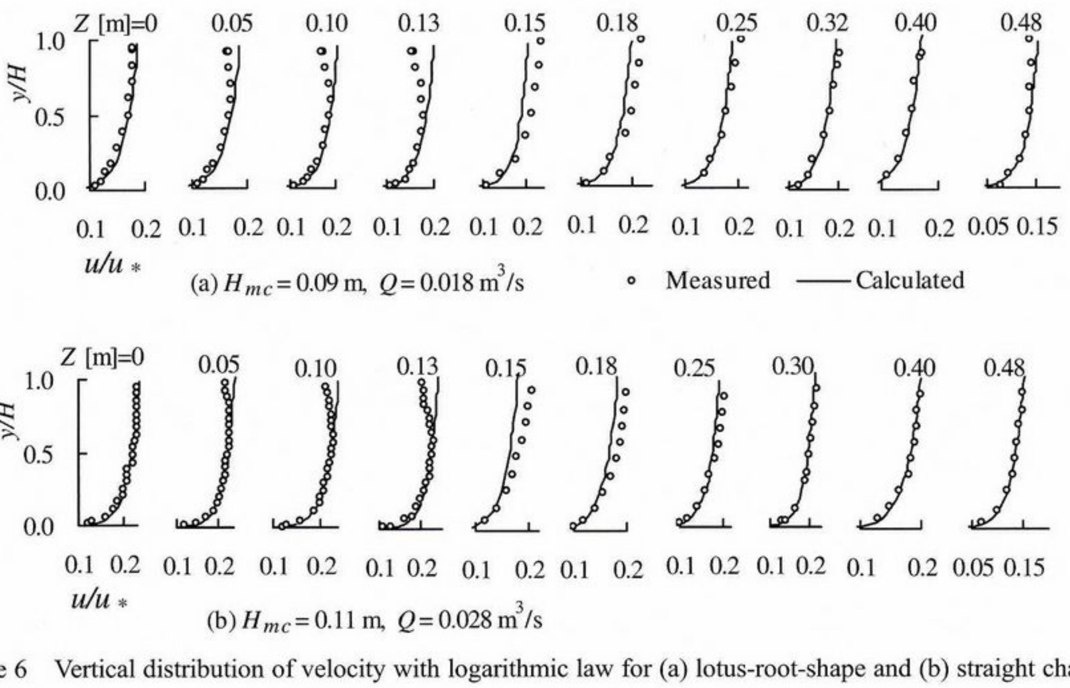

Figure 6 Vertical distribution of velocity with logarithmic law for (a) lotus-root-shape and (b) straight channel

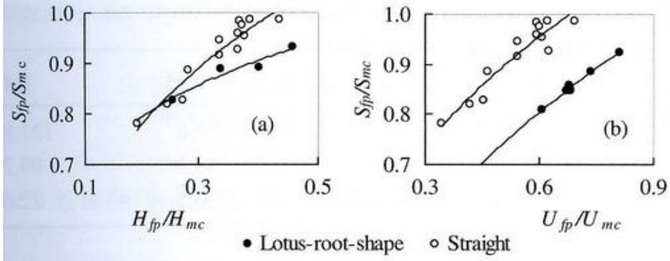

igure 7 Relationships for relative sediment concentration versus relative (a) flow depth and (b) velocity

epth H_{fp}/H_{mc} are shown in Fig. 7. Here S_{fp} and S_{mc} are the sediient concentrations in the floodplain and the main channel, espectively. The relative sediment concentrations in the two ompound channels increase with relative velocity and flow epth. The relative sediment concentration increases with relative epth more rapidly in the straight than in the lotus-root-shape hannel. The relative sediment concentration increases with relave velocity at similar rates for the two compound channels.

The vertical distributions of sediment concentration in the vo compound channels change with the flow momentum xchange (Fig. 8). A distortion of the vertical distribution in ıe interface region between the main channel and the floodplain apparent, and cannot be predicted by the formula of Rouse 1937). The measured sediment concentrations are smaller ıan the calculated values in the main channel. In other egions, the distortion remains small, and the formula describes ıe experimental data.

Mean gradients of the sediment concentration in the vertical irection are given in Table 2. Their magnitude indicates the symmetry in the vertical distribution. The gradients in Table 2 are averages of all experimental data, namely $(S_b - S_s)/H$, where H is the flow depth in the main channel or in the floodplain, depending on the location of the measurement line, and S_b and S_s are the sediment concentrations at $0.1H$ and $0.9H$, respectively. For both compound channels, the mean gradients are smaller in the lotus-root-shape than in the straight channel, and are larger on the floodplain than in the main channel, respectively.

4 Theoretical analyses

4.1 *Divided mode of compound cross-section*

According to the flow characteristics for the two types of compound channels, the cross-section can be divided into four regions (Fig. 9): (I) undisturbed region of main channel (URMC), (II) interactive region between channel and plain (IRCP), (III) undisturbed region in the floodplain (URFP) and (IV) boundary region (BR). In the URMC and URFP, vertical distributions of velocity have a logarithmic component, and can be described as

$$\frac{u}{u_*} = M \lg \frac{y u_*}{v} + N, \tag{1}$$

where u is the flow velocity at position y, u_* the local shear velocity and coefficients M and N were calibrated by the experimental data, resulting in $M = 5.64$ and $N = 5.86$. In the BR, distributions of flow velocity are mainly affected by boundaries, and distributions are similar to those of the single open channel. In the IRCP, the interactive action of the flow momentum transfer

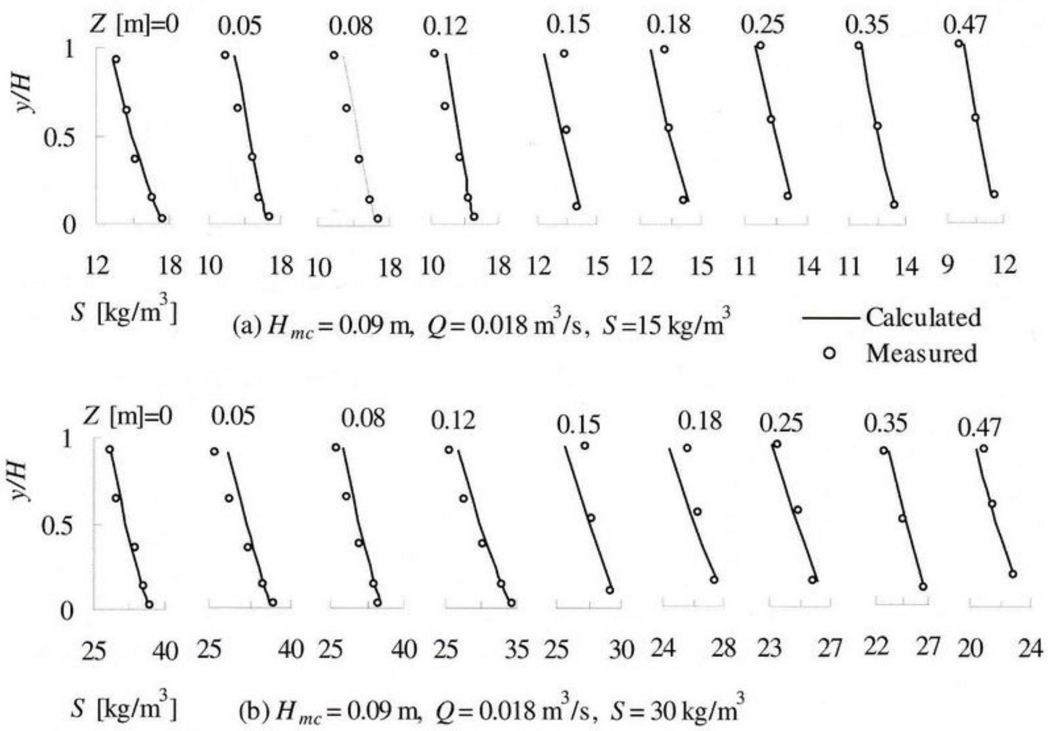

gure 8 Vertical distribution of sediment concentration compared with Rouse (1937) distribution for (a) lotus-root-shape channel, (b) straight channel

Table 2 Averaged gradients of sediment concentration in vertical direction (kg/m^3 m)

Distance (m)	0	0.08	0.12	0.15	0.25	0.35	
Straight channel	22.1	19.8	19.4	70.1	96.1	100.6	[illegible]
Lotus-root-shape channel	16.5	15.9	15.6	64.1	77.3	80.5	[illegible]
Difference	5.6	3.9	3.8	6.0	18.8	20.1	[illegible]

s strong, and the flow structure changes on a large scale. The width of each region can be described as (Fig. 9) $b_{\rm I} = 2(b_{mc} - b_{m0})$, $b_{\rm II} = b_{m0}+b_{f0}$, $b_{\rm III} = b_{fp} - b_{fb} - b_{f0}$, and $b_{\rm IV} = b_{fb}$. Here, $b_{\rm I}$, $b_{\rm II}$, $b_{\rm III}$ and $b_{\rm IV}$ are the widths of URMC, IRCP, URFP, and BR, respectively, b_{m0} is the width of the side of the main channel in IRCP, b_{f0} the width of the side of the floodplain in IRCP, b_{mc} and b_{fp} the half widths of the main channel and floodplain, respectively, and b_{fb} the width of the floodplain in the BR. The parameters b_{m0}, b_{f0} and b_{fb} were estimated from experimental data as (Rajaratnam and Ahmadi 1981, Wang 1984, Zhou 1995, Ji 1997)

$$\frac{b_{m0}}{h_d} = 2.16\left(\frac{H_{fp}}{H_{mc}}\right)^{0.392}\left(\frac{b_{fp}}{b_{mc}}\right)^{0.308} \quad (2)$$

$$\frac{b_{f0}}{h_d} = 2.35\left(\frac{H_{fp}}{H_{mc}}\right)^{0.245}\left(\frac{b_{fp}}{b_{mc}}\right)^{0.189} \quad (3)$$

$$\frac{b_{fb}}{h_d} = 2.37\left(\frac{H_{fp}}{h_d}\right)^{0.31} \quad (4)$$

4.2 *Verification of logarithmic formula in IRCP*

According to typical characteristics of the vertical velocity distribution, IRCP can be divided into two parts, namely the inner zone of the main channel, in which the velocity distribution follows a logarithmic formula as Eq. (1). The other is the outer zone in the floodplain, in which the velocity distribution follows a wake function as

$$\frac{u}{u_*} = 5.641g\frac{yu_*}{\nu} \quad Kf(y,z) + 5.86 \quad (5)$$

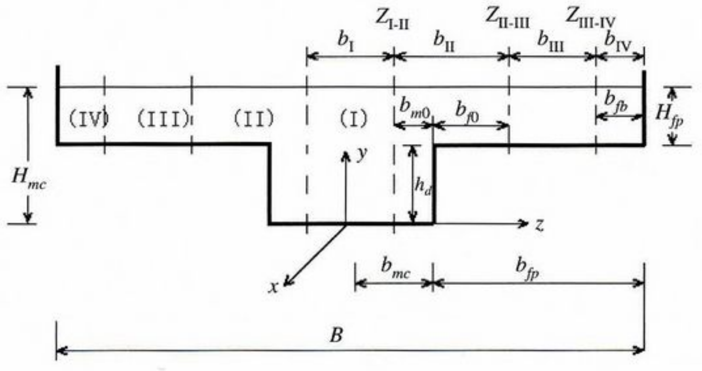

Figure 9 Sketch of divided cross-section for compound channel

in which

$$f(y,z) = \cos\left[\left(\frac{z - b_{mc}}{z_0 - b_{mc}}\right)\cdot\frac{\pi}{2}\right]\sin\left[\left(\frac{y}{h} - \phi\right)\cdot\frac{\pi}{2}\right],$$

where K is the coefficient describing the degree of momen exchange between the main channel and the floodplain value was calibrated using the test data, resulting in K -12.71 for the main channel and $K = 5.82$ for the floodp Therefore, the logarithmic formula in the outer zon described by

(1) For $\phi H_{mc} \le y \le H_{mc}$ and $z_{\rm I-II} \le z < b_{mc}$

$$\frac{u}{u*} = 5.64\,{\rm lg}\frac{yu_*}{\nu} - 12.71\cos\left[\left(\frac{z - b_{mc}}{z_{\rm I-II} - b_{mc}}\right)\cdot\frac{\pi}{2}\right] \times \sin\left[\left(\frac{y}{H_{mc}} - \phi\right)\cdot\frac{\pi}{2}\right] + 5.86$$

(2) For $\phi H_{fp} \le y \le H_{fp}$ and $b_{mc} \le z \le z_{\rm II-III}$

$$\frac{u}{u_*} = 5.64\,{\rm lg}\frac{yu_*}{\nu} + 5.82\cos\left[\left(\frac{z - b_{mc}}{z_{\rm II-III} - b_{mc}}\right)\cdot\frac{\pi}{2}\right] \times \sin\left[\left(\frac{y}{H_{fp}} - \phi\right)\cdot\frac{\pi}{2}\right] + 5.86$$

4.3 *Analytical solution for depth-averaged velocity in IR*

For a steady uniform turbulent flow, the momentum equati the streamwise direction is combined with the conti equation to give

$$\rho\left[\frac{\partial\overline{UV}}{\partial z} + \frac{\partial\overline{UW}}{\partial y}\right] = \rho gJ + \frac{\partial}{\partial z}\left(-\rho\overline{uv} + \mu\frac{\partial\overline{U}}{\partial z}\right) + \frac{\partial}{\partial y}\left(-\rho\overline{uw} + \mu\frac{\partial\overline{U}}{\partial y}\right),$$

where x, y, z are the streamwise, normal and lateral direct respectively, U, W, V the x, y, z components of the tem mean velocity, u, w, v the turbulent perturbations of vel with respect to the mean, J the slope, g the gravitational acce tion, and ρ and μ the density and dynamic viscosity, respecti The depth-averaged momentum equation is obtained egrating Eq. (9) over the flow depth using

$$\rho gHJ + \frac{\partial(H\overline{\tau}_{zx})}{\partial z} - \tau_b = \frac{\partial h(\rho\overline{UV})_d}{\partial z} \quad (10)$$

ere τ_b is the bed shear stress, and

$$\tau_b = \frac{f}{8}\rho U_d^2 \quad (11)$$

$$\overline{\tau}_{zx} = \frac{1}{H}\int_0^H \left(-\rho\overline{uv} + \mu\frac{\partial\overline{U}}{\partial z}\right) \mathrm{d}y \quad (12)$$

$$\left(\rho\overline{UV}\right)_d = \frac{1}{H}\int_0^H \rho\overline{UV}\,\mathrm{d}y \quad (13)$$

It is assumed that the secondary flow contribution is linear to HJ, i.e.

$$\frac{\partial H(\rho\overline{UV})_d}{\partial z} = \varphi\rho gHJ \quad (14)$$

l the depth-averaged transverse shear stress τ_{zx} is expressed in ns of the lateral gradient of depth-averaged velocity as

$$\overline{\tau}_{zx} = \rho\overline{\varepsilon}_{zx}\frac{\partial U_d}{\partial z} \quad (15)$$

The eddy viscosity ε_{zx} is often related to the local shear ocity $u_* = (\tau_b/\rho)^{1/2}$, depth H and the eddy viscosity coeffi- nt λ as

$$\overline{\varepsilon}_{zx} = \lambda H u_* = \lambda H\left(\frac{f}{8}\right)^{1/2} U_d \quad (16)$$

This coefficient is not constant in a compound channel, with maximum near the interface $z = b_{mc}$ (Xie 1980, Shiono and ight 1991, Zhou 1995). It varies further in the lateral direction he width of the main channel b_{mc}, or width b_{I} of IRCP. It is described herein as

$$\lambda = \left[\frac{\alpha(z - b_{mc})}{b_{\mathrm{I}}} + \beta\right]^2, \quad (1$$

where α and β are the constants determined from test da (Tominaga and Nezu 1991, Zhou 1995). For the main channe $\alpha_{mc} = 0.181$ and $\beta_{mc} = 0.563$. For the floodplain, $\alpha_{fp} = 0.46$ and $\beta_{fp} = 0.784$.

Substituting Eqs (14)–(17) into Eq. (10), and assuming U_d $= \eta_\xi$ and $\xi = \alpha(z-b_{mc})/b_{\mathrm{I}}+\beta$ for simplicity, gives a kind Bessel equation as (Wang and Guo 1979)

$$\xi^2\frac{\partial\eta_\xi}{\partial\xi^2} + 2\xi\frac{\partial\eta_\xi}{\partial\xi} + b_m\eta_\xi = 0 \quad (1$$

Thus, the transverse distribution of depth-averaged velocity the IRCP is

$$U_d^2 = \eta_\xi = A\xi^{-1+\Delta_u/2} + B\xi^{-1-\Delta_u/2} + CU^2, \quad (1$$

where U is the transect mean velocity, $\Delta_u{}^2 = 1+8b_{\mathrm{I}}{}^2(f/8)^{1/2}$ α^2H^2, and A, B and C the coefficients depending on the bounda conditions. Note from Fig. 10 that the calculated results fro Eq. (19) compare well with the measured data.

4.4 *Analytical solution of depth-averaged sediment concentration in IRCP*

The distribution of suspended sediment concentration was dete mined by considering the sediment mass balance under the infl ence of diffusive and convective transport. In general, for stea and uniform flow, if sediment transport is in an equilibrium sta in the streamwise direction, the diffusive equation describi sediment concentration is simplified to (Chien and Wan 1999)

$$\frac{\partial}{\partial y}\left(\varepsilon_{sy}\frac{\partial S}{\partial y}\right) + \frac{\partial}{\partial z}\left(\varepsilon_{sz}\frac{\partial S}{\partial z}\right) + \frac{\partial}{\partial y}(\omega S) = 0, \quad (2$$

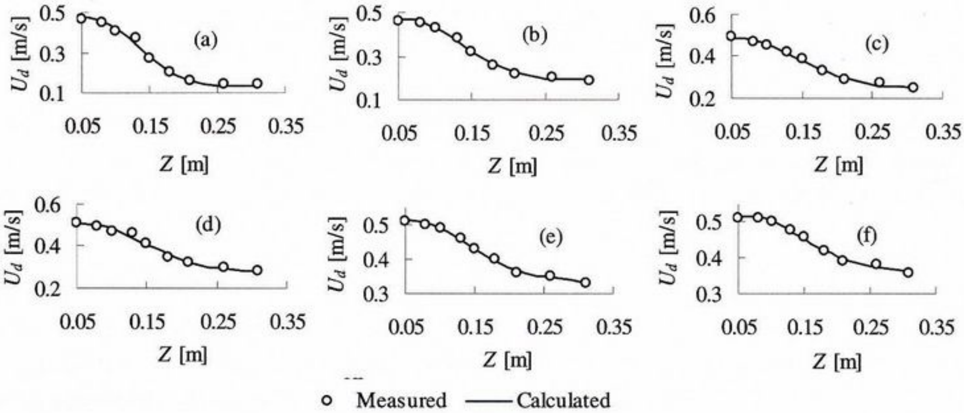

re 10 Comparison of calculated and measured results for velocity $U_d(Z)$ and H_{mc} (m) = (a) 0.07, (b) = 0.08, (c) = 0.09, (d) = 0.10, (e) = 0. (f) = 0.12

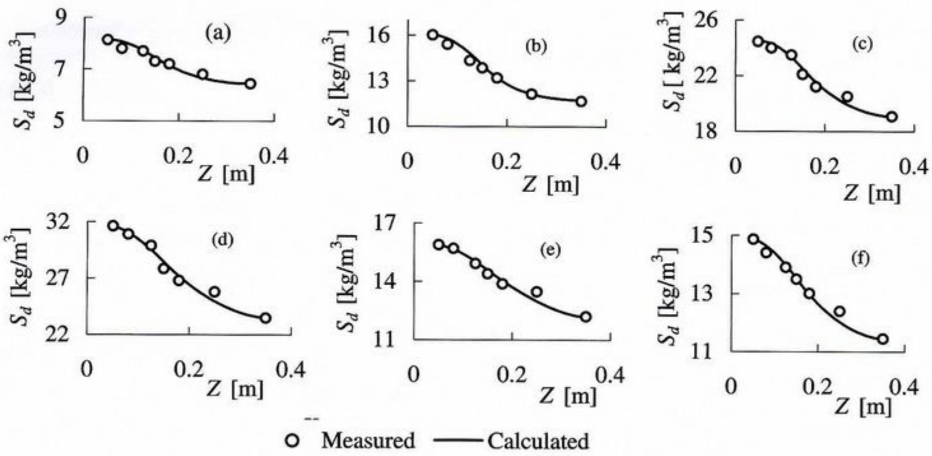

Figure 11 Comparison of calculated and measured sediment concentrations $S_d(Z)$ for H_{mc} (m) = (a) 0.09, (b) = 0.08, (c) = 0.09, (d) = 0.09, (
0.10 and (f) = 0.09

where ε_{sy} and ε_{sz} are the diffusive coefficients in y and z directions, respectively, and ω the fall velocity. Equation (20) is integrated over the flow depth to give

$$\left(\varepsilon_{sy}\frac{\partial S}{\partial y}+\omega S\right)\Big|_{\delta}^{H}+\frac{\partial}{\partial z}\left(\varepsilon_{sz}\frac{\partial HS_d}{\partial z}\right)=0, \qquad (21)$$

where S_d is the depth-averaged sediment concentration and δ the distance from the bed to the bottom of the turbulent layer.

Because there is no sediment transfer across the water surface, the boundary condition requires

$$\left(\varepsilon_{sy}\frac{\partial S}{\partial y}+\omega S\right)\Big|_{y=H}=0 \qquad (22)$$

At the plain bed, the rate of sediment transport across the boundary is defined as the probability that a particle reaching the bed will deposit. The boundary condition for sediment transport on the bed is described as

$$\left(\varepsilon_{sy}\frac{\partial S}{\partial y}+\omega S\right)\Big|_{y=\delta}=\omega_b(S_b-S_{bc}) \qquad (23)$$

Assuming that the sediment transport rate on the bed is linear to the depth-averaged rate, i.e. $\omega_b S_b=\lambda_1\omega_d S_d$, and the sediment transport capacity has a similar relationship $\omega_b S_{bc}=\lambda_2\omega_d S_{dc}$, then by combining Eqs (21)–(23), Eq. (20) is simplified as

$$\frac{\partial}{\partial z}\left(\varepsilon_{sz}\frac{\partial HS_d}{\partial z}\right)-\lambda_1\omega_d S_d+\lambda_2\omega_d S_{dc}=0, \qquad (24)$$

where S_b, ω_b and S_{bc} are the sediment concentration, fall velocity and bed transport capacity, respectively, and S_d, ω_d and S_{dc} the depth-averaged sediment concentration, fall velocity and transport capacity, respectively.

The transverse disperse coefficient is assumed to have same structure as the transverse eddy coefficient, namely

$$\varepsilon_{sz}=\varepsilon_{zx}=HU\left(\frac{f}{8}\right)^{1/2}\left[\frac{\alpha(z-b_{mc})}{b_{\mathrm{I}}}+\beta\right]^2 \qquad ($$

Substituting Eq. (25) into Eq. (24) and assuming that $\xi =$ $-\ b_{mc})/b_{\mathrm{I}}+\beta$, the transverse distribution of the depth-avera sediment concentration in IRCP is

$$S_d=A\xi^{-1+\Delta_s/2}+B\xi^{-1-\Delta_s/2}+CS_c, \qquad ($$

where S_c is the transect mean concentration, Δ_s $1+4\lambda_1\omega_d b_{\mathrm{I}}^2(f/8)^{1/2}/\alpha^2H^2U$, and A, B and C are coeffici determined from the boundary conditions (if $z=z_{\mathrm{I-II}}$, $z_{\mathrm{II-III}}$ and $z=b_{mc}$, S_d and $\partial S_d/\partial z$ are continuous). The calcul results and measured data are found to be very similar (Fig. However, differences between the simulated and measured c centrations are observed in IRCP, because Eq. (26) may reasonably simulate the sediment transport in that region to the complex flow-sediment exchange between the n channel and floodplain.

5 Conclusions

An experimental study on the flow movement and the sedin transport is presented relating to a straight and a lotus-root-sh compound channel. Using model experimentation, the main f characteristics can be summarized as follows:

(1) The flow conveying capacity is smaller in the straight c pound channel than in the single channel, but larger tha the lotus-root-shape compound channel.
(2) The compound cross-section can be divided into regions in terms of flow movement and sediment transp They comprise the (I) undisturbed region in the n channel, (II) interactive region between the channel

plain, (III) undisturbed region in the floodplain and (IV) boundary region. The width of each region was determined from measured data.

In both undisturbed regions (I and III), the vertical distribution of longitudinal velocity still obeys a logarithmic law, and the Rouse formula can be used for sediment concentration. There are differences in the vertical distributions of longitudinal velocity and sediment concentration between measurements and predictions in the interactive region (II), however.

A revised logarithmic formula is proposed using a wake function for the characteristics of the vertical velocity distribution. Based on the simplified momentum and diffusion equations, empirical expressions for the eddy and diffuse coefficients were given. Expressions to predict the transverse distributions of the depth-averaged velocity and sediment concentration are also specified. The results agree well with the measured data in the interactive region.

knowledgements

s research was financially supported by the National Science d for Distinguished Young Scholars (50725930) and Science d for Creative Research Groups (50721006).

tation

= width of compound channel (m)
= width of main channel (m)
= widths of URMC, IRCP, URFP and BR, respectively (i = I, II, III and IV) (m)
= side width of main channel in IRCP (m)
= side width of floodplain in IRCP (m)
= half width of main channel (m)
= half width of floodplain (m)
= width of floodplain in BR (m)
= median diameter of sediments (m)
= Froude number in floodplain
= Froude number in main channel
= gravitational acceleration (m/s^2)
= flow depth of floodplain (m)
= flow depth of main channel (m)
= $H_{mc} - H_{fp}$ (m)
= channel bottom slope
= discharge (m^3/s)
= Reynolds number in floodplain
= Reynolds number in main channel
= suspended sediment concentration (kg/m^3)
= depth-averaged sediment concentration (kg/m^3)
= sediment-carrying capacity (kg/m^3)
= suspended sediment concentration in floodplain (kg/m^3)

S_{mc} = suspended sediment concentration in main channel (kg/m^3)
S_b = suspended sediment concentration near bed (kg/m^3)
S_{bc} = sediment-carrying capacity concentration near bed (kg/m^3)
S_s = suspended sediment concentration near free surface (kg/m^3)
U = transect mean velocity (m/s)
U_{fp} = flow velocity of floodplain (m/s)
U_{mc} = flow velocity of main channel (m/s)
u = flow velocity at position y (m/s)
u_* = shear velocity (m/s)
U, V, W = temporal-mean velocities in x, z, y directions, respectively (m/s)
u, v, w = turbulent perturbations of velocity in x, z, y directions, respectively (m/s)
U_d = depth-averaged flow velocity in IRCP (m/s)
x = distance in streamwise direction (m)
y = distance in normal direction from bed (m)
z = distance in transverse direction (m)
α, β = coefficients
ε = eddy viscosity (kg/m/s)
ϕ = flow depth coefficient
ρ = water density (kg/m^3)
μ = dynamic viscosity coefficient of water (kg/m/s)
ν = kinematic viscosity (m^2/s)
τ = bed shear stress (N/m^2)
ρ = density of water (kg/m^3)
ω = sediment settling velocity (m/s)

References

Chien, N., Wan, Z. (1999). *Mechanics of sediment transport*. ASCE, Reston, VA.

Ervine, D.A., Baird, J.I. (1982). Rating curves for rivers with overbank flow. *Proc. Inst. Civ. Eng*. 2(73), 456–472.

Fukuhara, T., Murota, A. (1990). Discharge assessment in compound channel with floodplain roughness. Intl. Conf., *River Flood Hydraulics*, Wallingford, UK, 153–162.

James, C.S. (1985). Sediment transfer to overbank sections. *J. Hydraulic Res*. 23(5), 435–452.

Ji, Z.W. (1997). Experimental study on flow and sediment transport in compound channel. *Master thesis*. China Institute of Water Resources and Hydropower Research, Beijing, China [in Chinese].

Knight, D.W., Shiono, K. (1990). Turbulence measurements in a shear layer region of a compound channel. *J. Hydraulic Res*. 28(2), 175–196.

Liu, B.Y. (1991). Study on sediment transport and bed evolution in compound channels. *PhD dissertation*. Kyoto University, Kyoto.

Myers, W.R.C. (1978). Momentum transfer in a compound channel. *J. Hydraulic Res.* 16(2), 139–150.

Myers, W.R.C., Elsawy, E.M. (1975). Boundary shear in channel with flood-plain. *J. Hydraul. Div. ASCE* 101(7), 993–946.

Prinos, P., Townsend, R.D. (1984). Comparison of methods for predicting discharge in compound open channels. *Adv. Water Res.* 7(2), 180–187.

Rajaratnam, N., Ahmadi, R. (1981). Hydraulics of channels with flood-plains. *J. Hydraulic Res.* 19(1), 43–60.

Rhodes, D.G., Knight, D.W. (1994). Velocity and boundary shear in a wide compound duct. *J. Hydraulic Res.* 32(5), 743–764.

Rouse, H. (1937). Modern conceptions of the mechanics of fluid turbulence. Paper No. 1965. *Trans. ASCE* 102, 463–505.

Shiono, K., Knight, D.W. (1991). Turbulent open-channel flows with variable depth across the channel. *J. Fluid Mech.* 222, 617–646.

Tominaga, A., Nezu, I. (1991). Turbulent structure in compound open-channel flow. *J. Hydraul. Eng.* 117(1), 21–41.

Tominaga, A., Nezu, I., Nagao, M. (1993). Hydraulic characteristics of flow in compound channels with rough floodplain. Proc. 25th *IAHR Congress A, Flood and Drought*, To Japan, 137–149.

Wormleaton, P.R., Allen, J., Hadjipanos, P. (1982). Disch assessment in compound channel flow. *J. Hydraul. ASCE* 108(9), 975–993.

Wormleaton, P.R., Merrett, D.J. (1990). An improved me of calculation for steady uniform flow in prisn main channel/floodplain sections. *J. Hydraulic Res.* 2 157–174.

Wang, S.D. (1984). Flow structure and suspend load in c pound channel. *Master thesis*. Wuhan University, China Chinese].

Wang, Z.X., Guo, D.R. (1979). *Panorama of special func* Science Press, Beijing, China, [in Chinese].

Xie, H.Q. (1980). Characteristics of overbank flow and hydr calculation. Proc. 1st Intl. Symp. *River Sedimentation*, G ghua Press, Beijing, China, 231–237, [in Chinese].

Zhou, Y.L. (1995). Experimental study of flow moveme compound channel of meandering river. *Master th* Wuhan University. China, [in Chinese].